The 2013 World Congress on
Advances in Structural Engineering and Mechanics (ASEM13)
Jeju, Korea, September 8-12, 2013

The Mechanical Behavior and Buckling Failure of Sharp-Notched SUS 304 Stainless Steel Tubes Subjected to Pure Bending Creep

* Kuo-Long Lee[1] and *Wen-Fung Pan[2]

[1] Department of Innovative Design and Entrepreneurship Management, Far East University, Tainan 744, Taiwan
[2] Department of Engineering Science, National Cheng Kung University, Tainan 701, Taiwan
[2] z7808034@email.ncku.edu.tw

ABSTRACT

In this study, the response of sharp-notched SUS 304 stainless steel tubes with notch depths of 0.2, 0.4, 0.6, 0.8 and 1.0 mm subjected to pure bending creep are investigated. The pure bending creep is to bend the tube to a desired moment and hold that moment for a period of time. From the experimental result, the creep curvature and ovalization increase with time. In addition, higher held moment leads to the higher creep curvature and ovalization of the tube's cross-section. Due to the increasing of the ovalization, the tube will buckle eventually. Finally, the formulation proposed Lee (2002) was modified for simulating the first and second stages of the creep curvature–time relationship for pure bending creep. Through comparing with the experimental finding, the theoretical analysis can reasonably describe the experimental result.

1. INTRODUCTION

In early stage, Kyriakides and his co-workers designed and constructed a tube cyclic bending machine, and conducted a series of experimental and theoretical investigations. Shaw (1985) investigated the inelastic behavior of 6061-T6 aluminum and 1018 steel tubes subjected to cyclic bending. Kyriakides (1987) extended the analysis of 6061-T6 aluminum and 1018 steel tubes to the stability conditions under cyclic bending. Corona (1988) investigated the stability of 304 stainless steel tubes subjected to combined bending and external pressure. Corona (1991) was the first to experimentally investigate the response of circular tubes under curvature-controlled cyclic bending with a non-zero mean curvature.

Recently, Pan and his co-workers also constructed a similar bending machine with a newly invented curvature-ovalization measurement apparatus (COMA), which was

[1] Professor
[2] Professor

designed and set up by Pan (1998) to study various kinds of tubes under different cyclic bending conditions. Lee (2001) studied the influence of the D_o/t (outside diameter/wall thickness) ratio on the response and stability of circular tubes subjected to symmetrical cyclic bending. Lee (2004) experimentally investigated the effects of the D_o/t ratio and curvature-rate on the response and stability of circular tubes subjected to cyclic bending. Chang (2008) experimentally and theoretically investigated the effect of the mean moment on the response and collapse of thin-walled tubes subjected to cyclic bending. Chang (2009) discussed the estimation of the buckling life of circular tubes subjected to cyclic bending.

In practical industrial applications, tubes are under the sea, so salt water can corrode the tube surface and produce notches. The mechanical behavior and buckling failure of a notched tube differs from that of a tube with a smooth surface. In 2010, Lee (2010) studied the variation in ovalization of sharp-notched circular tubes subjected to cyclic bending. Lee (2010) investigated the mechanical behavior and buckling failure of sharp-notched circular tubes under cyclic bending. Lee (2013) experimentally discussed the viscoplastic response and collapse of sharp-notched circular tubes subjected to cyclic bending.

However, the mechanical behavior and buckling failure of notched circular tube subjected to pure bending creep have not been investigated. The pure bending creep is to bend the tube to a desired moment and hold that moment for a period of time. Although Pan (1998) studied the effect of the prior curvature-rate at the preloading stage on the subsequent creep or relaxation behavior and Lee (2002) investigated the response of circular tubes with different D_o/t ratios subjected to pure bending creep, all results are considered the smooth circular tubes without any notch.

In this study, the response and collapse of sharp-notched SUS 304 stainless steel tubes subjected to pure bending creep are discussed. A four-point bending machine was used to conduct the sharp-notched SUS 304 stainless steel tubes. A curvature-ovalization measurement apparatus (COMA) designed and reported previously by Pan (1998) was used to control the curvature. For sharp-notched tubes, five different notch depths, 0.2, 0.4, 0.6, 0.8 and 1.0 mm, were considered in this study. The magnitude of the bending moment was measured by two load cells mounted in the bending device, and the magnitudes of the curvature and ovalization of the tube’s cross-section were measured by COMA.

2. EXPERIMENT

Sharp-notched SUS 304 stainless steel tubes with five different notch depths were subjected to pure bending creep by using a tube-bending device and a curvature-ovalization measurement apparatus in this study. Detailed descriptions of the device, apparatus, materials, specimens and test procedures are given as follows.

2.1 Bending Device

Fig. 1 shows a picture of the bending device. It is designed as a four-point bending machine, capable of applying bending and reverse bending. The device consists of two rotating sprockets resting on two support beams. Heavy chains run around the sprockets and are connected to two hydraulic cylinders and load cells forming a closed loop. Each tube is tested and fitted with solid rod extension. The contact between the tube and the rollers is free to move along axial direction during bending. The load transfer to the test specimen is in the form of a couple formed by concentrated loads from two of the rollers. Once either the top or bottom cylinder is contracted, the sprockets are rotated, and pure bending of the test specimen is achieved. Reverse bending can be achieved by reversing the direction of the flow in the hydraulic circuit. Detailed description of the bending device can be found in Kyriakides (1987) and Pan (1998).

Fig. 1 A picture of the bending device

The two sprockets rest on two heavy support beams 1.25 m apart. This allows a maximum length of the test specimen to be 1 m. The bending capacity of the machine is 5300 N-m. Each tube is tested and fitted with a solid rod extension. The contact between the tube and the rollers is free to move along the axial direction during bending. The load transfer to the test specimen is a couple formed by concentrated loads from two of the rollers. The applied bending moment is directly proportional to the tension in the chains.

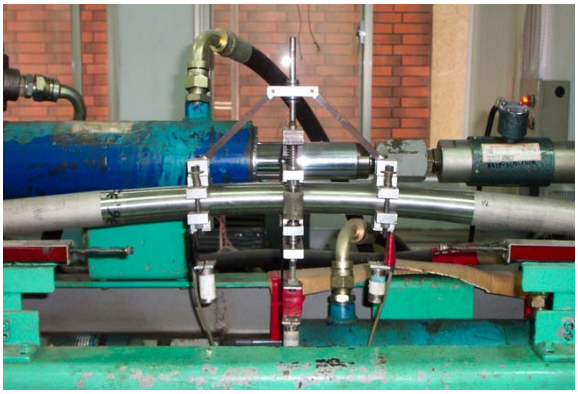

Fig. 2 A picture of the COMA

2.2 Curvature-Ovalization Measurement Apparatus (COMA)

Fig. 2 shows a picture of the COMA. The COMA is an instrument which can be used to measure the tube curvature and ovalization of the tube cross-section (Pan 1998). It is a lightweight instrument, which can be mounted close to the tube mid-span. There are three inclinometers in COMA. Two of them are fixed on two holders, which are denoted as side-inclinometers. The holders are fixed on the circular tube before the test begins. Based on the fixed distance between the two side-inclinometers and the angle changes detected by the two side-inclinometers, the tube curvature can be obtained by simple calculation (Pan 1998).

In addition, a magnetic detector in the middle part of the COMA was used to measure the change of the outside diameter. For measuring the change of the outside diameter at the sharp-notched tip, upper and lower magnetic blocks were set up with sharp probes on both magnetic blocks, as shown in Fig. 3. The tip of the probe can touch the sharp-notched tip, thus, the change of the outside diameter at the sharp notch can be measured.

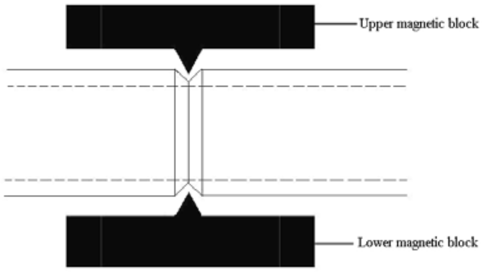

Fig. 3 Sharp probes on the upper and lower magnetic blocks

2.3 Materials and Specimens

Circular tubes made of SUS 304 stainless steel were used in this study. The tubes' chemical composition is Cr (18.36%), Ni (8.43%), Mn (1.81%), Si (0.39%), …., and a few other trace elements, with the remainder being Fe. The ultimate stress, 0.2% strain offset the yield stress and the percent elongation are 626 MPa, 296 MPa and 35%, respectively.

The raw unnotched SUS 304 stainless steel tubes had an outside diameter of 31.8 mm and wall thickness of 1.5 mm. The raw tubes were machined on the outside surface to obtain the desired shape and depth of the sharp notch. Fig. 4 shows a schematic drawing of the sharp-notched tube where the notched depth and width are denoted as and a and b. In this study, five different notch depths were considered including 0.2, 0.4, 0.6, 0.8 and 1.0 mm, respectively. However, the notch width was a constant magnitude of 0.4 mm for all sharp-notched tubes.

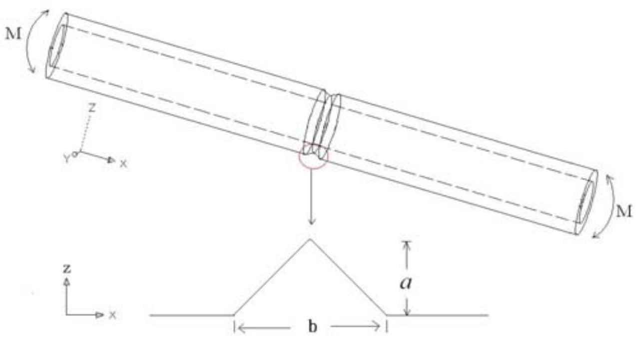

Fig. 4 A schematic drawing of the sharp-notched tube

2.4 Test Procedures

The test involved pure bending creep. For each notch depth, different magnitudes of moment were held for pure bending creep. The curvature-rate of the bending test was 0.003 $m^{-1}s^{-1}$. The magnitude of the bending moment was measured by two load cells mounted in the bending device. The magnitudes of the curvature and ovalization of the tube cross-section were measured by the COMA. In addition, the time for pure bending creep was also recorded.

3. EXPERIMENTAL RESULTS AND DISCUSSION

3.1 Experimental Response of Sharp-notched SUS 304 Stainless Steel Tubes under Pure Bending

Fig. 5 shows the experimentally determined moment (M) - curvature (κ) curves for sharp-notched SUS 304 stainless steel tubes with different a under pure bending. It can be seen that a tube with a higher value of a has a smaller wall-thickness. Thus, a lower magnitude of the moment is found when the tube bends to the maximum curvature. Fig. 6 depicts the corresponding experimental ovalization of the tube's cross-section ($\Delta D_o/D_o$) as a function of the applied curvature (κ) for Fig. 5. The ovalization is defined as $\Delta D_o/D_o$ where D_o is the outside diameter and ΔD_o is the change in the outside diameter. It can be seen that the ovalization increases with the amount of curvature. In addition, higher a of the notch tube causes greater ovalization of the tube's cross-section.

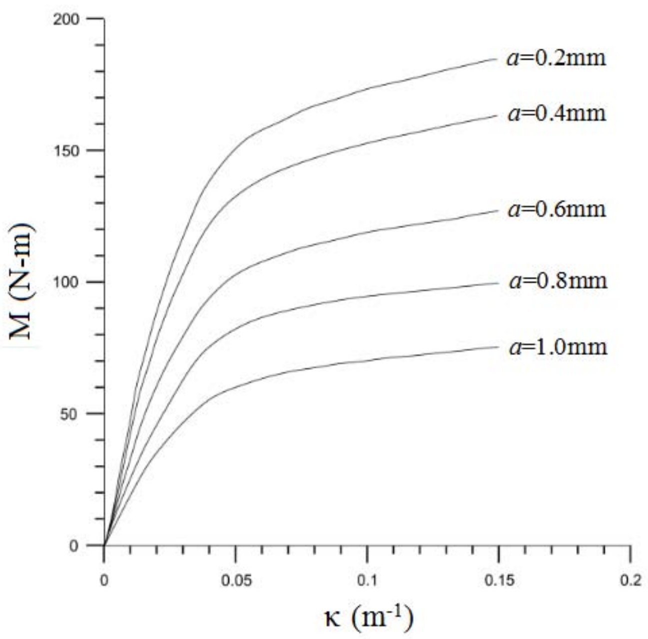

Fig. 5 The experimental moment (M) - curvature (κ) curves for sharp-notched SUS 304 stainless steel tubes with different a under pure bending

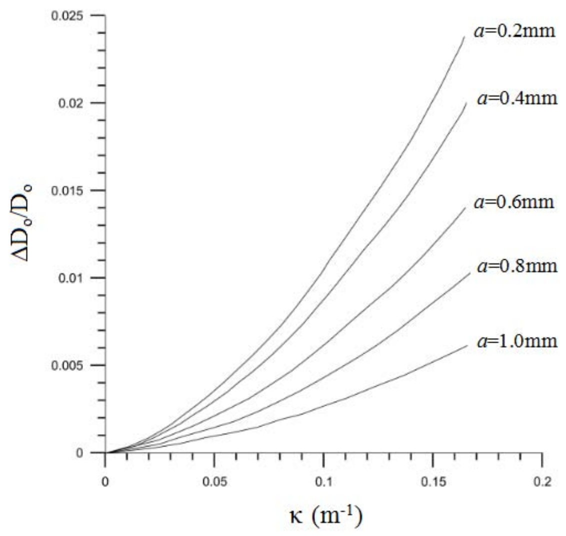

Fig. 6 The corresponding experimental ovalization ($\Delta D_o/D_o$) - curvature (κ) curves for sharp-notched SUS 304 stainless steel tubes with different a under pure bending

3.2 Experimental Response and Collapse of Sharp-notched SUS 304 Stainless Steel Tubes under Pure Bending Creep

Fig. 7 depicts the experimental curvature (κ) – time ($\bar{t}$) curves under pure bending and subsequent pure bending creep for sharp-notched SUS 304 stainless steel tube with a = 0.2 mm. The starting and buckling points of the pure bending creep are marked by "●" and "×", respectively. It can be seen that as soon as the creep starts the tube curvature quickly increases. Higher held moment leads to the higher creep curvature. Owing to the continuously increasing curvature, the tube buckles eventually.

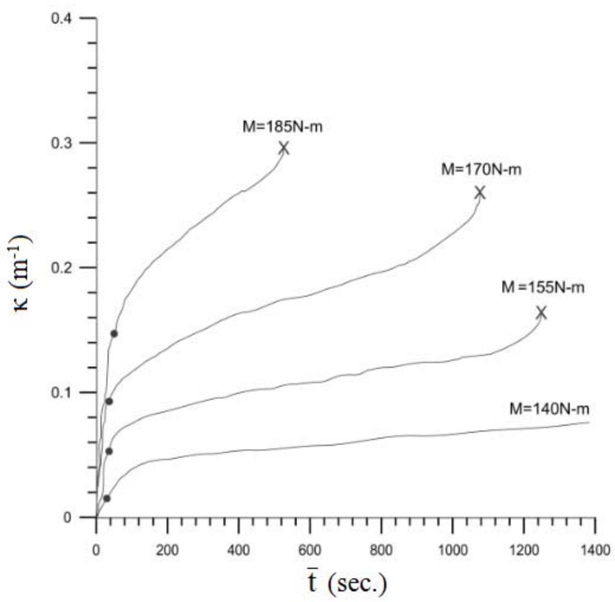

Fig. 7 The experimental curvature (κ) – time ($\bar{t}$) curves under pure bending and subsequent pure bending creep for sharp-notched SUS 304 stainless steel tube with a = 0.2 mm

We now consider the pure bending creep stage of Fig. 7 from the starting point"●" to the buckling point "×". A typical result of the creep curvature (κ_c) – time ($\bar{t}$) with the held moment of 155 N-m is shown in Fig. 8. It can be observed that the creep process, like smooth tube under pure bending creep tested by Lee (2002), has three stages: initial, secondary and tertiary stages. Once the pure bending creep starts, the magnitude of κ_c increases (the initial stage). When the amount of κ_c increases steadily with time, the pure bending creep enters the secondary stage. The tertiary stage is the final stage of the pure bending creep. In this stage, the rate of the κ_c increases drastically and buckling of the tube occurs.

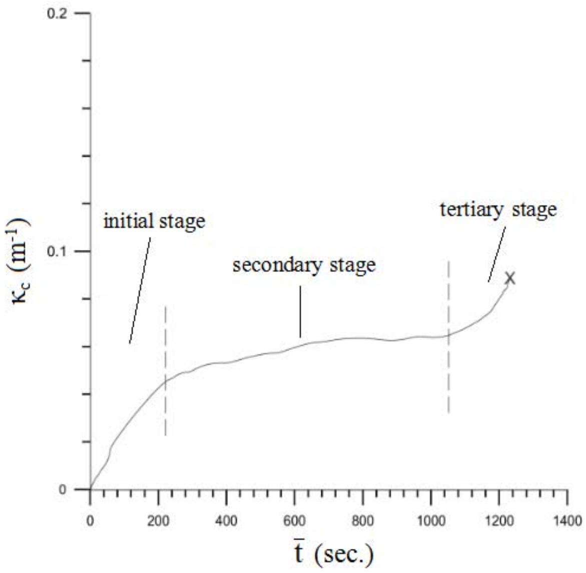

Fig. 8 The creep curvature (κ_c) – time ($\bar{t}$) curve with the held moment of 155 N-m

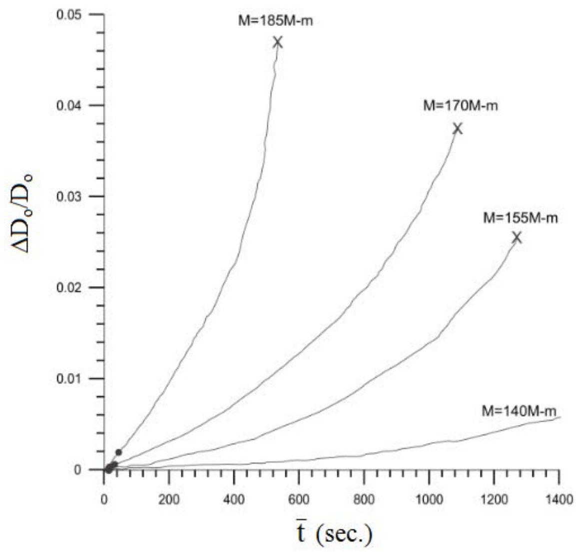

Fig. 9 The corresponding experimental ovalization ($\Delta D_o/D_o$) – time ($\bar{t}$) curves under pure bending and subsequent pure bending creep for Fig. 7

Fig. 9 shows the corresponding experimental ovalization ($\Delta D_o/D_o$) – time ($\bar{t}$) curves under pure bending and subsequent pure bending creep for Fig. 7. The starting and buckling points of the pure bending creep are also marked by "●" and "×", respectively. It can be seen that the curves are strongly influenced by the held moment for creep stage. The ovalization-rate for higher held moment is larger than that for lower held moment. In addition, the ovalizations at buckling for these four magnitudes of held moment are different. Higher held moment leads to the higher ovalization at buckling. This phenomenon is different from the result tested by Lee (2002) for smooth SUS 304 stainless steel tubes under pure bending creep. To highlight the influence of the sharp-notched depth, tubes with a = 0.4, 0.6, 0.8 and 1.0 mm were also tested. The phenomenon of the κ-$\bar{t}$ and $\Delta D_o/D_o$–$\bar{t}$ curves under pure bending creep was found to be very similar to the phenomenon of tubes with a = 0.2 mm.

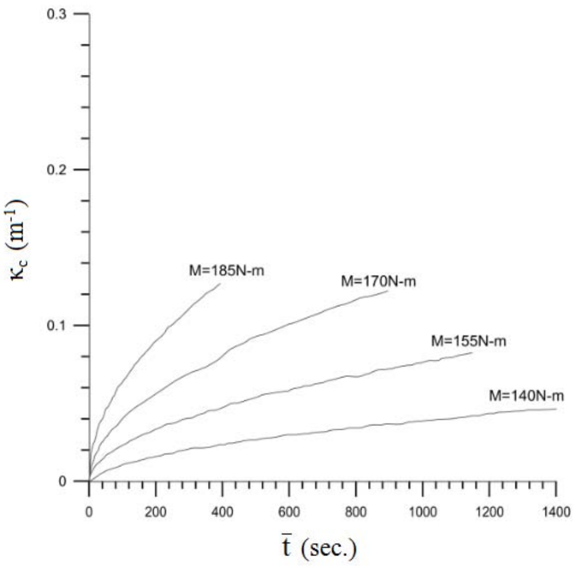

Fig. 10 The experimental κ_c-$\bar{t}$ curves for sharp-notched SUS 304 stainless steel tubes with a = 0.2 mm under pure bending creep in the initial and secondary stages

3.3 Theoretical Formulation for Sharp-notched SUS 304 Stainless Steel Tubes under Pure Bending Creep

Because most of the time for pure bending creep spends in the initial and secondary stages, the proposed theoretical formulation is only applicable in these two stages. Fig. 10 shows the experimental κ_c-$\bar{t}$ curves for sharp-notched SUS 304 stainless steel tubes with a = 0.2 mm under pure bending creep in the initial and secondary stages. In addition, the κ_c-$\bar{t}$ curves for sharp-notched SUS 304 stainless steel tubes with a = 0.4, 0.6, 0.8 and 1.0 mm under pure bending creep in the initial and secondary stages have similar trend as the sharp-notched tubes with a = 0.2 mm. The experimental results are shown in Figs. 13-16 in dotted lines. Since the trend of κ_c-$\bar{t}$ curves for sharp-notched circular tubes is very similar the trend of smooth circular tubes, thus, the formulation proposed by Lee (2002) was used in this investigation. The formulation proposed by them is

$$\kappa_c = C M^m \bar{t}^{\,n} \tag{1}$$

where M is the held moment, C, m and n are material parameters for pure bending creep. Due to the same material and same loading condition tested by Lee (2002), the material parameters m and n are the same amounts as they proposed to be 5.7 and 0.53, respectively. In this study, the parameter C is a function of notch depth a and wall thickness t. By curve fitting with the experimental data, the amounts of C for a/t = 0.133, 0.267, 0.400, 0.533 and 0.667 are 1.028×10^{-15}, 5.027×10^{-15}, 4.712×10^{-14}, 4.232×10^{-13} and 8.591×10^{-12}, respectively. If we consider the relationship between $\log C$ and a/t, a straight line can be used to describe the relationship (see Fig. 11). Therefore, parameter C is proposed to be

$$\log C = b_1 (a/t) + b_2 \tag{2}$$

where b_1 and b_2 are material parameters for pure bending creep which can be determined from Fig. 11 to be 7.012 and -16.133, respectively. The simulated results for sharp-notched SUS 304 stainless steel tube for a = 0.2, 0.4, 0.6, 0.8 and 1.0 mm under pure bending creep are demonstrated in Figs. 12-16, respectively, in solid lines. Good agreement between the experimental and theoretical results has been achieved.

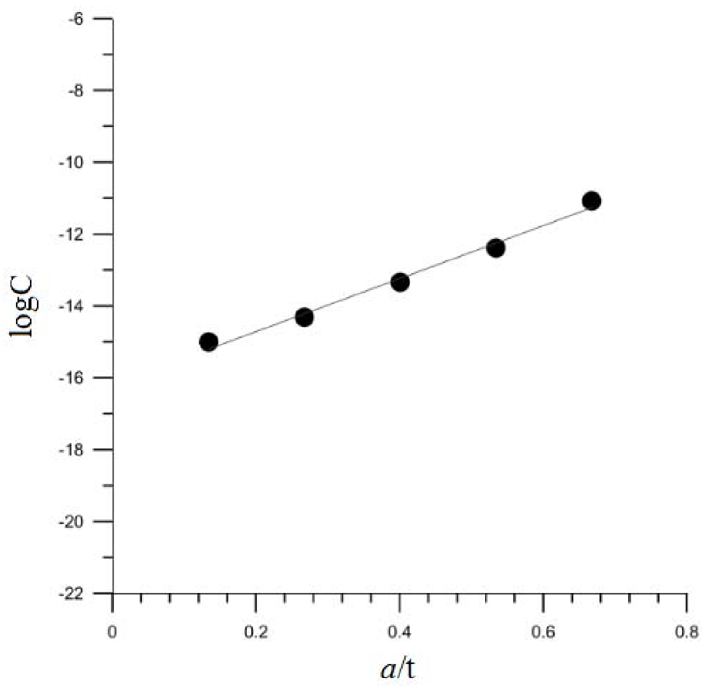

Fig. 11 The relationship between $\log C$ and a/t

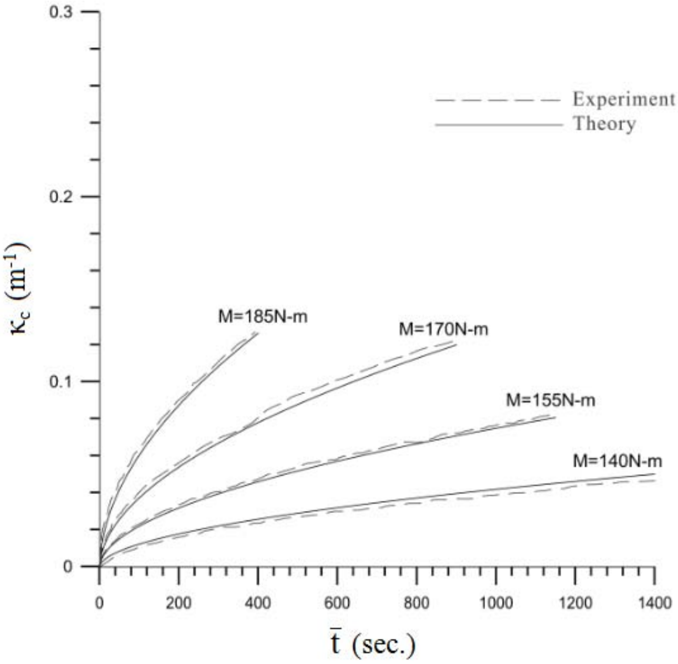

Fig. 12 The experimental and simulated κ_c- $\bar{t}$ curves for sharp-notched SUS 304 stainless steel tubes with a = 0.2 mm under pure bending creep in the initial and secondary stages

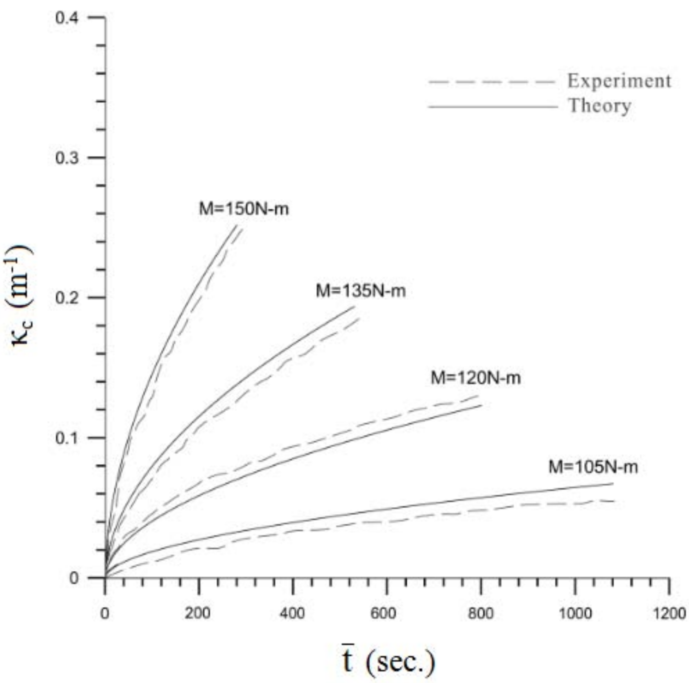

Fig. 13 The experimental and simulated κ_c- $\bar{t}$ curves for sharp-notched SUS 304 stainless steel tubes with a = 0.4 mm under pure bending creep in the initial and secondary stages

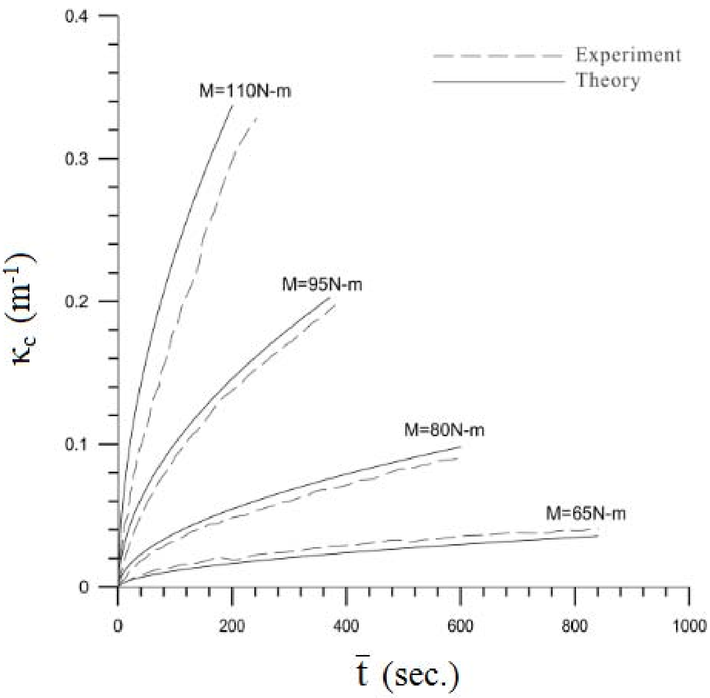

Fig. 14 The experimental and simulated κ_c- $\bar{t}$ curves for sharp-notched SUS 304 stainless steel tubes with a = 0.6 mm under pure bending creep in the initial and secondary stages

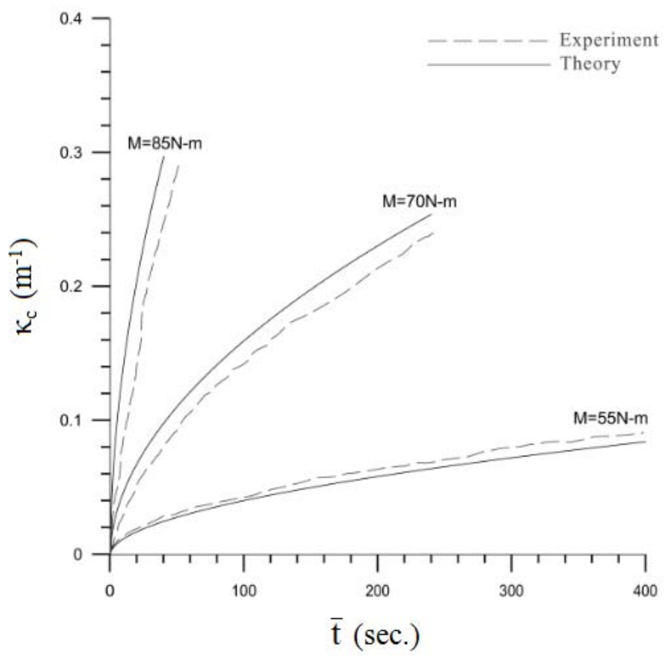

Fig. 15 The experimental and simulated κ_c- $\bar{t}$ curves for sharp-notched SUS 304 stainless steel tubes with a = 0.8 mm under pure bending creep in the initial and secondary stages

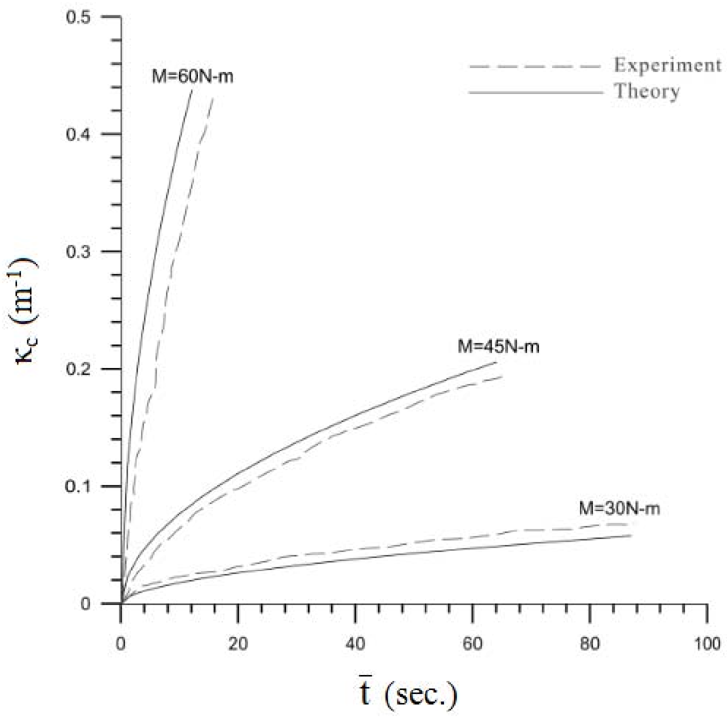

Fig. 16 The experimental and simulated κ_c- $\bar{t}$ curves for sharp-notched SUS 304 stainless steel tubes with a = 1.0 mm under pure bending creep in the initial and secondary stages

4. CONCLUSIONS

The mechanical behavior and buckling failure of the sharp-notched SUS 304 stainless steel tubes with different notch depths subjected to pure bending creep are experimentally and theoretically investigated in this study. Based on the experimental and theoretical results, the following important conclusions can be drawn:

(1) For pure bending, it is found from the M-κ curves that a tube with a higher value of a has a smaller wall-thickness. Thus, a lower magnitude of the moment is found when the tube bends to the maximum curvature. In addition, from the $\Delta D_o/D_o$-κ curves, the ovalization increases with the amount of curvature. Higher a of the notch tube causes greater ovalization of the tube's cross-section.

(2) For pure bending creep, higher held moment leads to the higher creep curvature and ovalization. Due to increasing of the tube's ovalization, the tube buckles eventually. In addition, the κ_c- $\bar{t}$ curve can be divided into three stages: initial, secondary and tertiary stages. Most of the time for pure bending creep spends in the initial and secondary stages.

(3) The theoretical formulation for smooth circular tube under pure bending creep proposed by Lee (2002) is modified so that it can be used for simulating the κ_c- $\bar{t}$ curve for sharp-notched circular tube under pure bending creep in the initial and secondary stages. Through comparison with the experimental data, the theoretical formulation

can properly simulate the experimental result.

5. ACKNOWLEDGEMENT

The work presented was carried out with the support of the National Science Council under grant NSC 100-2221-E-006-081. Its support is gratefully acknowledged.

REFERENCES

Chang, K.H. and Pan, W.F. (2009), “Buckling life estimation of circular tubes under cyclic Bending”, *Int. J. Solids Struct.*, **46**, 254-270.

Chang, K.H., Pan, W.F. and Lee, K.L. (2008), “Mean moment effect of thin-walled tubes under cyclic bending”, *Struct. Engng. Mech.*, **28**(5), 495-514.

Corona, E. and Kyriakides, S. (1988), “On the collapse of inelastic tubes under combined bending and pressure”, *Int. J. Solids Struct.*, **24**(5), 505-535.

Corona, E. and Kyriakides, S. (1991), “An experimental investigation of the degradation and buckling of circular tubes under cyclic bending and external pressure”, *Thin-Walled Struct.*, **12**, 229-263.

Kyriakides, S. and Shaw, P.K. (1987), “Inelastic buckling of tubes under cyclic loads”, *ASME J. Press. Vessel Technol.*, **109**, 169-178.

Lee, K.L. (2010), “Mechanical behavior and buckling failure of sharp-notched circular tubes under cyclic bending”, *Struct. Engng. Mech.*, **34**(3), 367-376.

Lee, K.L. and Pan, W.F. (2002), “Pure bending creep of SUS304 stainless steel tubes”, *Steel & Comp. Struct.*, **2**(6), 461-474.

Lee, K.L., Hsu, C.M. and Pan, W.F. (2013), “Viscoplastic collapse of sharp-notched circular tubes under cyclic bending”, *Acta Mech. Solida Sinica*, to be published.

Lee, K.L., Hung, C.Y. and Pan, W.F. (2010), “Variation of ovalization for sharp-notched circular tubes under cyclic bending”, *J. Mech.*, **26**(3), 403-411.

Lee, K.L., Pan, W.F. and Hsu, C.M. (2004), “Experimental and theoretical evaluations of the effect between diameter-to-thickness ratio and curvature-rate on the stability of circular tubes under cyclic bending”, *JSME International Journal, Series A*, **47**(2), 212-222.

Lee, K.L., Pan, W.F. and Kuo, J.N. (2001), “The influence of the diameter-to-thickness ratio on the stability of circular tubes under cyclic bending”, *Int. J. Solids Struct.*, **38**, 2401-2413.

Pan, W.F. and Fan, C.H. (1998), “An experimental study on the effect of curvature-rate at preloading stage on subsequent creep or relaxation of thin-walled tubes under pure bending”, *JSME International Journal, Series A*, **41**(4), 525-531.

Pan, W.F., Wang, T.R. and Hsu, C.M. (1998), “A curvature-ovalization measurement apparatus for circular tubes under cyclic bending”, *Experimental Mechanics*, **38**(2), 99-102.

Shaw, P.K. and Kyriakides, S. (1985), “Inelastic analysis of thin-walled tubes under cyclic bending”, *Int. J. Solids Struct.*, **21**(11), 1073-1110.